Atlas-Based Segmentation of Breast MR Images

Farzad Khalvati and Anne Martel

Sunnybrook Research Institute
Toronto, Ontario, Canada
www.sunnybrook.ca/research

Abstract. This paper presents a new pipeline for the segmentation of breast in 3D MR images which can be used to calculate breast density; an important risk factor in determining the possibility of breast cancer. We propose an efficient atlas-based segmentation algorithm that classifies atlas images based on local phase information and uses groupwise registration to create centroid for each class. To segment a target image, it is first determined which class it belongs to. Next, a nonrigid registration is used to align the target image and centroid of the class in order to generate the segmentation result. The proposed algorithm was applied to 400 MRI datasets (350 for training and 50 for testing) and an average Dice coefficient (DSC) of 0.93 was achieved.

Keywords: Breast MRI segmentation, image registration, groupwise registration, phase congruency, image classification

1 Introduction

Magnetic resonance imaging (MRI) of breast is increasingly becoming a common approach for monitoring and detection of breast cancer mainly due to higher sensitivity and no ionizing radiation compared to conventional x-ray mammography. The segmentation of breast tissue in MR images is a crucial task in the analysis of patient data because it makes the 3D visualization possible without the clutter of unimportant structures such as heart obscuring the breast tissue. This is useful in monitoring breast cancer where MR imaging is now also recommended for screening women who are known to be at a higher risk of breast cancer [1]. In addition, it is necessary to segment breast images prior to breast density calculation which is a significant risk factor and an important biomarker in determining the possibility of breast cancer [2]. Moreover, Computer-Aided Diagnosis (CAD) needs breast segmentation prior to performing an efficient auto-detection task and finally, breast segmentation is necessary prior to therapy planning where multiple segmentations of breast images such as CTV (Clinical Tumor Volume) and GTV (Gross Tumor Volume) are required. Atlas-based segmentation (ABS) is a well established and widely used technique for extracting contours from medical images. In this method, processed images are stored in a database or an atlas along with their optimal segmentation results (i.e., manual segmentation or label). A target image is usually registered to the atlas and the label of the atlas is deformed using the registration transformation. In general, there are two approaches to design an ABS algorithm: probabilistic atlas [3] and multi-atlas [4] approaches, where in the former, a probability map of images in the atlas is created and registered to the target image and in the latter, the labels of multiple images in the atlas contribute to generating the segmentation result for the target image. The Multi-atlas approach is usually computationally expensive limiting its practicality. A multi-atlas approach for segmenting pectoral muscle in breast MRI was proposed in [5] where all images in the atlas were registered and compared to the target image and the deformed labels of the best-match images were selected and fused using the method proposed in [4] to yield the final segmentation result.

In this paper, we present a new multi-atlas approach for fully automatic segmentation of breast MR images. It combines image classification and mean image building to create an efficient atlas that while producing highly accurate results, it incurs a reasonable computational cost.

2 Methods

In a multi-atlas approach, the goal is to increase the accuracy of the results by diversifying the atlas (i.e., atlas selection). However, bigger atlases[1] make ABS computationally expensive. We use a pre-processing stage to create local phase maps of images in the atlas (section 2.1), based on which the images are clustered. We use groupwise registration (section 2.2) to create a centroid image[2] for each class which is used for registering to the target image. We present the proposed algorithm in section 2.3 followed by results and discussion in sections 3 and 4, respectively. Section 5 concludes the paper.

2.1 Phase Congruency Map (PCM)

The information about the local phase of an image can be used to detect structural characteristics of the image in a way that is invariant to image intensity. The main idea behind phase congruency is that the Fourier components of an image are all in phase (congruent) where there is a meaningful edge in the image.

Equation 1 calculates the phase congruency of an image at location x ($PC(x)$) where $E(x)$ is local energy of the image, T is a threshold to suppress the effect of noise on the local energy of the image at that location, A_n represents the amplitude of the n^{th} Fourier component, and ϵ is set to a small number to avoid division by 0 [6]. In order to implement phase congruency, a bank of quadrature filters with different spatial frequencies (e.g., Log Gabor filters) are used [6] [7].

$$PC(x) = \frac{\lfloor E(x) - T \rfloor}{\Sigma_n A_n(x) + \epsilon} \tag{1}$$

[1] We refer to images used in training as *atlas* and hence, an atlas may contain one image or multiple images.

[2] Centroid image of each class has minimum dissimilarity from all images in the class.

Workshop on Breast Image Analysis
In conjunction with MICCAI 2013

2.2 Groupwise Image Registration

In contrast to pairwise registration where every image in the population is registered to a reference image, groupwise registration transforms a group of images into a reference image such that the dissimilarity between the reference image and each image in the group is minimal. A reference image which has already been manually segmented, plays a crucial role in ABS methods in which it is registered to the target image. In practice, however, generating a reference image is not straight forward; even with careful atlas selection, the selected image may not represent the population well enough and hence, the registration may not produce acceptable results. The advantage of using groupwise registration versus pairwise registration for atlas generation is that a sophisticated mean image that represents all images in the group is automatically generated without being biased toward a specific image in the population. Groupwise registration aligns a set of images to a virtual reference image by generating a set of transformations that map the reference image to each of the images in the group. Balci et al. [8] proposed a framework for groupwise registration of images where it uses the stack entropy cost function and a multi-resolution B-spline non-rigid deformation to generate the set of image transformations. The motivation behind using stack entropy as cost function was that by aligning the images accurately, the intensity values of pixels in the corresponding locations in the stacked images should not vary significantly, which means that the stack entropy should be low [8]. The proposed approach uses a combination of global and local transformations where the former is an affine transformation and the latter is a nonrigid deformation based on B-splines [9].

2.3 Proposed Algorithm

The proposed algorithm in this paper consists of two stages namely training (or atlas building) and testing. The algorithm is applied to 3D breast MR images and therefore, all the intermediate stages (e.g., creating PCMs, clustering, and registration etc.) are performed on 3D images.

Training The training data consists of images with the manual segmentation for whole breast. In order to have a diverse atlas with a reasonable size to manage computationally, we cluster the training images into different classes based on the similarity of the corresponding PCMs. The PCMs of images in the training data are compared (using correlation coefficient) pairwise to create a (dis)similarity matrix. The similarity matrix is fed to a multidimensional scaling (MDS) algorithm [10] to create a 2D distance map of PCMs of all images. The K-means algorithm [11] is used to cluster images into different classes based on the distance map of the corresponding PCMs.

At this point, each class consists of several images and the corresponding PCMs along with the labels. First, we use groupwise registration (section 2.2) to register all the PCMs in each class together to create the representative PCM for each class. Afterward, we apply groupwise registration to the original images in

ISBN: 978-87-996443-0-8

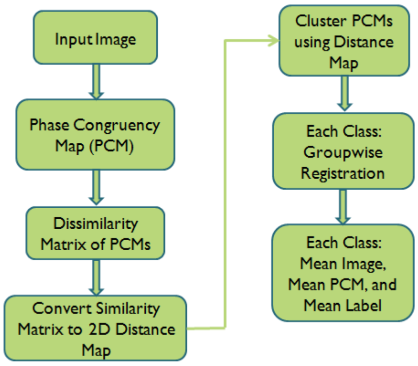

Fig. 1. Training

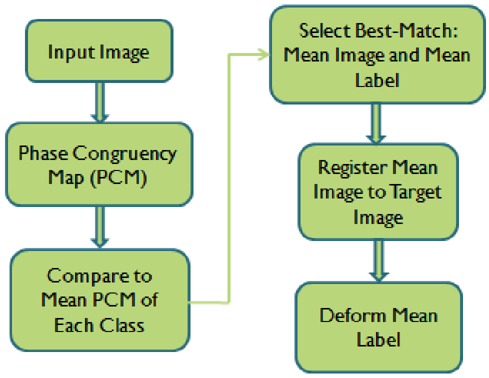

Fig. 2. Testing

each class to create the mean image and the corresponding mean label. For each class of images in the atlas, this gives a representative PCM, a mean image (or centroid), and mean label to be used for segmenting the target image (Figure 1).

Test When an unseen image (target image) arrives, first, its PCM is created and compared to the representative PCMs of all classes. Once the best-match class is found, the corresponding mean image is registered to the target image via a nonrigid registration algorithm using elastix [12]. The registration transformation is then applied to the mean label of the best-match class to create the segmentation result for the target image (Figure 2).

2.4 Materials

The training and test data, used from a previous study [13], contained 400 breast MRI datasets ($94 \times 94 \times 44$ pixels) of Dixon imaging sequence (used for water and fat separation) manually segmented by an expert to mark the boundaries of breast. The population consisted of two age groups; 320 women aged 15-30 and 80 women aged 40-60. Out of 400 MRI datasets, 350 datasets were used to create the atlas (280 datasets from the younger and 70 datasets from the older group) and 50 datasets were used to generate breast volume using the proposed algorithm to evaluate performance (40 datasets from the younger and 10 datasets from the older group).

3 Results

To evaluate the performance of the proposed algorithm, the segmentation results for the entire volume were compared to the ground-truth results (i.e., manual

ISBN: 978-87-996443-0-8

Workshop on Breast Image Analysis
In conjunction with MICCAI 2013

segmentation) using Dice Similarity Coefficient (DSC) and Jaccard index[3]. The best configuration of the algorithm (i.e., 20 classes of images in the atlas) yielded mean DSC and Jaccard index of 93%±5% and 87±8%, respectively. The median values for the DSC and the Jaccard index were 94% and 89%, respectively. Figure 3 shows a sample test image, the corresponding best-match atlas, and the segmentation result for a single slice. Figure 4 shows the distribution of the segmentation accuracy for all 50 patients test data. To segment a target MR image volume, it took 2 min on Intel(R) Core(TM)2 i5 CPU 3.33GHz.

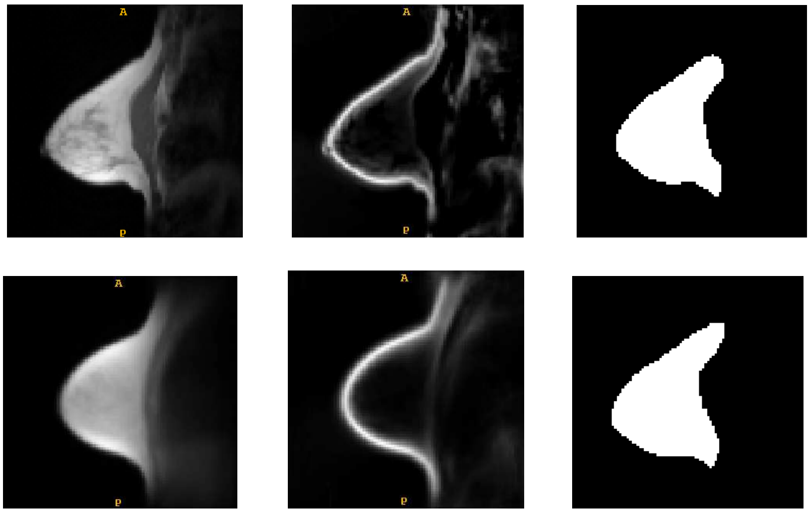

Fig. 3. Top - Target image (left to right): original image, PCM, ground-truth result. Bottom - (left to right): best-match centroid, best-match PCM, segmentation result.

4 Discussion

The proposed algorithm classifies the training images, based on the similarity of the corresponding PCMs, using K-means algorithm. The target image's PCM is compared to the representative PCMs of all classes and the best-match centroid (or mean image) is selected to be registered to the target image. With respect to image registration terminology, the target image is in fact the *fixed* image $F(x)$ and the best-match centroid is the *moving* image $M(x)$ with mean label $M'(x)$. By registering $M(x)$ to $F(x)$, we obtain a transformation $y(x)$ which yields:

$$M(y(x)) \approx F(x) \tag{2}$$

[3] For two sets A and B, DSC and Jaccard index are defined as $\frac{2|A \cap B|}{|A|+|B|}$ and $\frac{|A \cap B|}{|A \cup B|}$, respectively.

Applying the transformation $y(x)$ to the mean label of the best-match centroid $M'(x)$ produces $M'(y(x))$. The closer $M'(y(x))$ to the actual label of $F(x)$ (i.e., $F'(x)$), the higher the accuracy of the segmentation results will be. The number of classes is expected to influence the overall performance of the algorithm. To investigate this, we ran experiments for different numbers of classes in the atlas (i.e., 1 class to 75 classes) with the same training and test data as described in section 2.4.

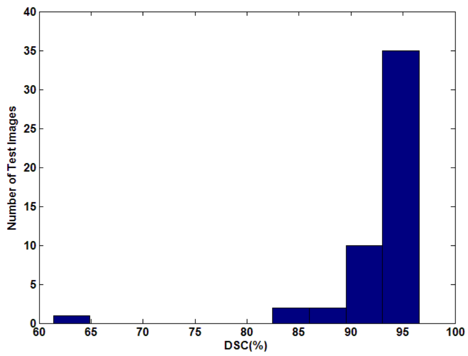

Fig. 4. DSC value comparison between the segmentation and ground-truth results

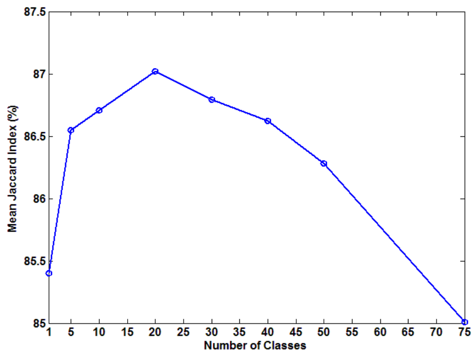

Fig. 5. Algorithm performance with respect to the number of classes in the atlas

Figure 5 shows the mean Jaccard index values for the test data for different numbers of classes used to classify the training images. It is interesting to observe that there is an optimal number of classes of images[4] (i.e., 20) that yields the best results in terms of the accuracy of the proposed algorithm. The first phenomenon that affects the performance of the proposed algorithm is the fact that when registering the best-match centroid $M(x)$ to the target image $F(x)$, for a fixed number of iterations of the cost function's optimizer, the more similar $M(x)$ and $F(x)$, the higher the similarity of the transformed $M(x)$ and $F(x)$ will be (i.e., higher $sim(M(y(x)), F(x))$). This will lead to a more accurate segmentation result (i.e., higher $sim(M'(y(x)), F'(x))$).

From K-means classification it is known that the more the number of classes, the higher the similarity of a new random variable to the best-match centroid will be. This is, in general, true because as the number of classes increases, the error of clustering (i.e., dissimilarity between target image and centroid of best-match class) should decrease because clusters are smaller. We ran an experiment

[4] The optimal number of classes may be different for different training/test images.

for different numbers of classes and it was confirmed that the higher the number of classes of atlas images, the more similar the best-match centroid image was to the target image (Figure 6), which means higher $sim(M(x), F(x))$.

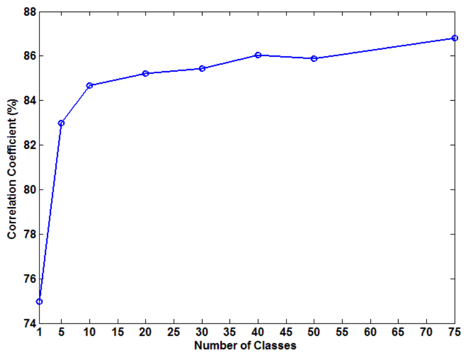

Fig. 6. Similarity of target image vs. best-match centroid

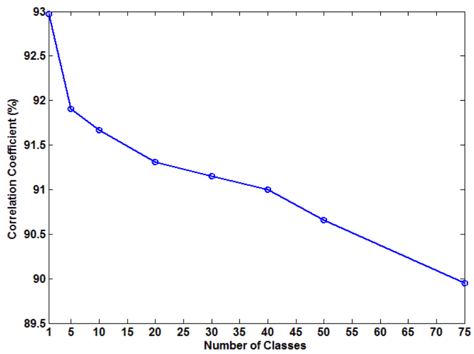

Fig. 7. Similarity of best-match centroid vs. its label

Another phenomenon that affects performance of the algorithm with respect to the number of classes (Figure 5) is the amount of similarity between the best-match centroid and its label. When registering $M(x)$ to $F(x)$, all pixels in $M(x)$ are considered. In order to obtain the segmentation result, the transformation obtained by registering $M(x)$ to $F(x)$, $y(x)$, is applied to a fraction of pixels in $M(x)$ which has been binarized (i.e., the label or $M'(x)$). Thus, the more similar $M(x)$ and $M'(x)$, the more accurate the result of applying $y(x)$ to $M'(x)$ will be (i.e., higher $sim(M'(y(x)), F'(x))$).

For a fixed number of training images (e.g., 350), increasing the number of classes decreases the average number of images per class. When registering a larger population of images in one class using groupwise registration, there is a higher chance that the mean image (i.e., centroid) converges toward the region(s) of interest (i.e., label). This may be due to the fact that the region(s) of interest in the image contain(s) less randomness in their texture in comparison to the background. We ran an experiment for different numbers of classes and it was confirmed that the higher the number of classes (i.e., fewer images per class), the less similar the centroid image was to its corresponding label (Figure 7)[5].

The two phenomena discussed above contribute to the behaviour of the proposed algorithm in which there is an optimal number of classes that yields the best accuracy for the segmentation results (Figure 5).

[5] The similarity of two images was calculated by correlation coefficients.

ISBN: 978-87-996443-0-8

5 Conclusion

A new multi-atlas-based segmentation algorithm was presented where atlas images are clustered based on local phase maps and each class centroid is created using groupwise registration. The proposed algorithm generates highly accurate results for segmentation of breast MR Dixon images with a reasonable computational cost. As future work, local phase maps of training images will be directly used to create an atlas that is intensity invariant. An ABS algorithm will be developed in which the intensity-invariant atlas created from Dixon images will be used to segment other MR image sequences such as T1 and T2.

References

1. Warner E.: The role of magnetic resonance imaging in screening women at high risk of breast cancer. Top Magn Reson Imaging. 19(3):163-9 (2008)
2. Boyd, N., Guo, H., Martin, L., Sun, L., Stone, J., Fishell, E., Jong, A., Hislop, G., Chiarelli, A., Minkin, S., Yaffe, M.: Mammographic density and the risk and detection of breast cancer. N. Engl. J. Med. 356, 227236 (2007)
3. Martin, S., Troccaz, J., Daanen, V.: Automated segmentation of the prostate in 3D MR images using a probabilistic atlas and a spatially constrained deformable model, Med. Phys., Vol. 37, pp. 1579-1590, 2010.
4. Klein, S., van der Heide, U., Lips, I., van Vulpen, M., Staring, M., Pluim, J.P.W.: Automatic segmentation of the prostate in 3d MR images by atlas matching using localized mutual information. Med. Phys. 35(4), 14071417 (2008)
5. Gubern-Mrida A., Kallenberg M., Mart R., Karssemeijer N.: Segmentation of the pectoral muscle in breast MRI using atlas-based approaches, Med. Image Comput. Comput. Assist. Interv. 15(Pt 2), 371-8 (2012)
6. Kovesi, P.: Phase congruency: a low-level image invariant. Psychological Research 64 (2), 136148 (2000)
7. Gallego Ortiz, C., Martel, A. L.: Automatic atlas-based segmentation of the breast in MRI for 3D breast volume computation. Med. Phys. 39 (10), 5835–5848. (2012)
8. Balci, S. K., Golland, P., Shenton, M., Wells, W.M.: Free-Form B-spline Deformation Model for Groupwise Registration. Int. Conf. Med. Image Comput. Comput. Assist. Interv. 10, 23–30.(2007)
9. Rueckert, D., Sonoda, L. I., Hayes, C., Hill, D. L. G., Leach, M. O., Hawkes, D. J.: Nonrigid registration using free-form deformations: Application to breast mr images. IEEE Tans. Med. Imaging 18 (9),712-721. (1999)
10. Steyvers, M.: Multidimensional Scaling. Multidimensional Scaling. Encyclopedia of Cognitive Science. (2006)
11. Lloyd, S. P.: Least squares quantization in PCM. IEEE Trans. Inf. Theory 28(2), 129136 (1982)
12. Klein., S., Staring, M., Murphy, K., Viergever, M. A., Pluim, J. P. W.: elastix: a toolbox for intensity based medical image registration. IEEE Trans. Med. Imaging, 29 (1), 196–205. (2010)
13. Boyd, N., Martin, L., Chavez, S., Gunasekara, A., Salleh, A., Melnichouk, O., Yaffe, M., Friedenreich, C., Minkin, S., Bronskill, M.: Breast-tissue composition and other risk factors for breast cancer in young women: A cross-sectional study, Lancet Oncol. 10, 569580 (2009)

ISBN: 978-87-996443-0-8